Simulation of carbon cycling, including dissolved organic carbon transport, in forest soil locally enriched with ^{14}C

E. Tipping · P. M. Chamberlain · M. Fröberg · P. J. Hanson · P. M. Jardine

Abstract The DyDOC model was used to simulate the soil carbon cycle of a deciduous forest at the Oak Ridge Reservation (Tennessee, USA). The model application relied on extensive data from the Enriched Background Isotope Study (EBIS), which exploited a short-term local atmospheric enrichment of radiocarbon to establish a large-scale manipulation experiment with different inputs of ^{14}C from both above-ground and below-ground litter. The model was first fitted to hydrological data, then observed pools and fluxes of carbon and ^{14}C data were used to fit parameters describing metabolic transformations of soil organic matter (SOM) components and the transport and sorption of dissolved organic matter (DOM). This produced a detailed quantitative description of soil C cycling in the three horizons (O, A, B) of the soil profile. According to the parameterised model, SOM turnover within the thin O-horizon rapidly produces DOM (46 gC m^{-2} a^{-1}), which is predominantly hydrophobic. This DOM is nearly all adsorbed in the A- and B-horizons, and while most is mineralised relatively quickly, 11 gC m^{-2} a^{-1} undergoes a "maturing" reaction, producing mineral-associated stable SOM pools with mean residence times of 100–200 years. Only a small flux (~1 gC m^{-2} a^{-1}) of hydrophilic DOM leaves the B-horizon. The SOM not associated with mineral matter is assumed to be derived from root litter, and turns over quite quickly (mean residence time 20–30 years). Although DyDOC was successfully fitted to C pools, annual fluxes and ^{14}C data, it accounted less well for short-term variations in DOC concentrations.

Keywords ^{14}C · Carbon · Cycling · Dissolved organic carbon · Dissolved organic matter · DyDOC model · Enriched Background Isotope Study · Litter manipulation · Soil

E. Tipping (✉) · P. M. Chamberlain
Centre for Ecology and Hydrology, Lancaster Environment Centre, Lancaster LA1 4AP, UK
e-mail: et@ceh.ac.uk

M. Fröberg
Department of Soil and Environment, SLU – Sveriges Lantbruksuniversitet, 7001, 750 07 Uppsala, Sweden

M. Fröberg · P. J. Hanson
Environmental Sciences Division, Oak Ridge National Laboratory, Oak Ridge, TN 37831-6422, USA

P. M. Jardine
Biosystems Engineering and Soil Science Department, Institute for a Secure and Sustainable Environment, University of Tennessee, Knoxville, TN 37996-4531, USA

Introduction

Transformations of soil organic matter (SOM) are important for the global carbon cycle, and affect the

functional properties of soil. Understanding and prediction of how they will respond to environmental change, particularly warming, require quantitative knowledge about soil C turnover, and this requires the construction of suitable models. The simplest treatment of SOM as a single pool characterised by a mean residence time may be useful for comparative purposes, but oversimplifies SOM heterogeneity (Trumbore 2000). Amundson (2001) suggested that a minimum of three pools with different turnover rates should be considered, characterised as "fast", "slow" and "passive", and the well-known models RothC (Jenkinson 1990) and CENTURY (Parton et al. 1987) operate at this level. More elaborate models take different soil horizons into account (Parton et al. 1998; Jenkinson and Coleman 2008), and include dissolved organic matter (DOM) transport and retention within the soil profile (Neff and Asner 2001; Michalzik et al. 2003).

Parameterisation of the more complex models requires considerable analytical data. For SOM these include concentrations and stocks, and specific pools derived from physical and chemical fractionation studies (e.g. Rumpel et al. 2004; Buurman and Jongmans 2005; Swanston et al. 2005; Mikutta et al. 2006). With regard to DOM, information on fluxes is needed, and fractionation is also informative (e.g. Qualls and Haines 1991), together with experimental studies in the laboratory (Guggenberger and Zech 1992; Qualls and Haines 1992; Kaiser and Zech 1997; Kalbitz et al. 2005) and the field (Fröberg et al. 2003, 2007a, b; Hagedorn et al. 2004; Kalbitz et al. 2007). The determination of the radiocarbon contents of SOM and DOM, combined with information on the changing atmospheric $^{14}CO_2$ signal, represents a vital non-invasive tool for the characterisation of turnover rates (Trumbore 2009).

Isotopic tracer applications are usually restricted to timescales of decades (bomb carbon) or centuries-to-millennia (radioactive decay), but application to shorter timescales has recently been made possible in the Enriched Background Isotope Study (EBIS; Trumbore et al. 2002; http://ebis.ornl.gov). The EBIS study took advantage of a large pulse of ^{14}C that effectively labelled substantial areas of deciduous forest at the Oak Ridge Reservation (ORR) in east Tennessee (USA), while leaving areas of similar forest nearly unaffected. EBIS quantified ^{14}C-enrichment and involved the translocation of ^{14}C-labelled litter from highly enriched areas to slightly

enriched ones, and vice versa, enabling the short-term dynamics of litter decomposition, including the production of "new" DOC, to be examined.

In the work described here, we used the wealth of field and analytical data produced in EBIS, and drew on the results of extensive studies of solute and DOC transport at ORR (Jardine et al. 2006), to parameterise the moderately complex mechanistic soil carbon model DyDOC (Michalzik et al. 2003) for the deciduous forest soils at ORR. The DyDOC model simulates DOM transport and retention in soils, in relation to the overall soil C cycle, making use of ^{14}C data for both SOM and DOM. Soil carbon cycling is described using a combination of up to five carbon pools per horizon, undergoing first-order metabolic transformations. DyDOC includes the production of DOC, its sorption to the soil solids, and DOC transport by percolating water through the soil profile. The model has so far been applied to spruce forests (Michalzik et al. 2003; Tipping et al. 2005) and grass moorland (Tipping et al. 2007), but only with fairly limited data.

The goal of the present work was to use EBIS data sets to test whether the assemblage of processes that constitute DyDOC can quantitatively explain the available observations of C dynamics for the ORR soils. More specifically, DyDOC was used to simulate and investigate the origins, dynamics and fate of DOM within the soil profile. A major objective was to determine if DyDOC model simulations would produce results consistent with experimental conclusions that DOM leaving the O-horizons of forest soils is predominantly formed from older material (Fröberg et al. 2003, 2007b; Kalbitz et al. 2007), while at the same time explaining the vertical migration of DOM from recent litter to considerable depth (70 cm) at ORR (Fröberg et al. 2007a). With respect to carbon accumulation in the mineral soils, there is growing evidence that DOM can be a significant source of stabilised (adsorbed) mineral soil carbon in forest soils (Baisden and Parfitt 2007; Kalbitz and Kaiser 2008; Sanderman and Amundson 2009); the DYDOC simulations presented here provide further insight into this process for upland soils of a deciduous forest.

The enriched background isotope study

Elevated levels of ^{14}C–CO_2 in the air and soil atmosphere at ORR were observed during the

summer of 1999. Local analyses determined that the elevated background ^{14}C-signature of soil-derived CO_2 was the result of a release of ^{14}C in the form of $^{14}CO_2$ gas from a local industrial incinerator (Trumbore et al. 2002). Hanson et al. (2005) further describe the uniqueness of this pulse and its application to experimental studies of soil carbon cycling. The enrichment of atmospheric CO_2 with locally released ^{14}C led to the labelling of the forest, and the incorporation of additional ^{14}C into plants, litter and soil (Trumbore et al. 2002; Swanston et al. 2005; Hanson et al. 2005). The main enrichment occurred in 1999, but there had been smaller events in preceding years. Enrichment was greater in the western part of the reservation.

The EBIS field sites were located on the U.S. Department of Energy's National Environmental Research Park near Oak Ridge, TN, USA (35°58′ N 84°16′ W). The research plots are located on up-slope, ridge-top positions, with slopes in the range 0–15°, in the upland oak forest type (*Quercus* spp.; *Acer* spp.) including scattered pine (*Pinus echinata* Mill. and *P. virginiana* Mill.), mesophytic hardwoods (*Liriodendron tulipifera* L., *Fagus grandifolia* J.F. Ehrh.), and some hickory (*Carya* spp.). The ages of the over-storey trees cover a broad range from about 40 to 150 years, and the maximum canopy height is approximately 26 m. Climate characteristics of the central ORR include annual precipitation of 1,390 mm, mean annual temperature of 14.5°C, and range 4–25°C (Johnson and Van Hook 1989; Hanson and Wullschleger 2003). Annual water loss due to evaporation and transpiration is ca. 650 mm (Luxmoore and Huff 1989). The soils (silt loams) are either Inceptisols derived from shale or Ultisols derived from dolomitic parent materials. The surface soils typically comprise a thin (ca. 3 cm) O-horizon, 15 cm A-horizon and 45 cm B-horizon. Soil pH is ca. 5. Further details of the soils are given by Wilson and Luxmoore (1988) and Jardine et al. (1988, 2006).

A detailed description of the EBIS experimental design is provided in Hanson et al. (2005), the following is a brief version. To facilitate EBIS, large quantities of leaf litter were collected from the west and east ends of the ORR during fall canopy senescence in 2000 when the 'natural' incorporation of the ^{14}C-signature was greatest. The collections included enriched ($\Delta^{14}C$ of ~1000‰) and near-background ($\Delta^{14}C$ of ~220‰) litter. These materials

were used for replicated studies of soil C cycling. Prior to leaf senescence in the fall of 2000, plastic tarps were laid out on the forest floor to collect enriched foliage in the vicinity of the 1999 ^{14}C release, and foliage representing near-background conditions away from the release at the east end of ORR. Litter was manually collected from the tarps weekly from September to mid-December 2000. The litter was dried and stored for future experimental use.

Four research sites were established on the ORR (See Fig. 1 of Hanson et al. 2005). Two 'enriched' sites at the west end were established on Ultisol and Inceptisol soils of Pine Ridge and on Tennessee Valley Authority land on Chestnut Ridge (TVA),
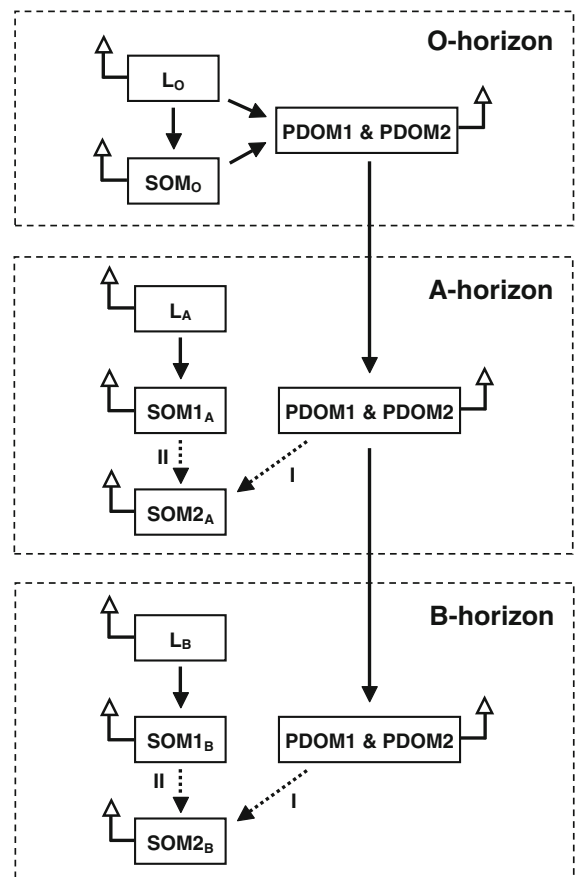

Fig. 1 Soil pools and transformations postulated in DyDOC-04. The *solid arrows* indicate metabolic transformation of organic matter or transport of DOM, the *open arrows* indicate release of CO_2. The *dotted lines* labelled I and II indicate alternative modes of formation of the high-density fraction of SOM. Key: *L* litter, *SOM* soil organic matter, *PDOM* potential dissolved organic matter; see the text for further details

respectively. Two 'near-background' sites were established approximately 10 km further east. The near-background sites included a site with Ultisols within Walker Branch Watershed on Chestnut Ridge, and a site with Inceptisols on Haw Ridge. At each of the four research sites on the ORR, eight 7×7 m plots were established. From late September to early December of 2000, the forest floor within each plot was covered with landscape cloth, and the ambient litterfall was periodically removed. After the landscape cloth was removed in mid-December, ^{14}C enriched or near-background litter was added back to the respective treatment plots at a rate of 500 g dry mass m^{-2}. The following combination of replicated research plots was created by the experimental design:

– BB near-background 2000 litter, background roots and soil C (Walker Branch and Haw Ridge, eastern ORR);
– BE near-background 2000 litter, ^{14}C-enriched root litter and soil C (Pine Ridge and TVA, western ORR);
– EB ^{14}C-enriched 2000 litter, background roots and soil C (Walker Branch and Haw Ridge, eastern ORR);
– EE ^{14}C-enriched leaf litter, ^{14}C-enriched root litter and soil C (Pine Ridge and TVA western ORR).

Samples of enriched and near-background litter and all organic and mineral soil samples were analyzed for ^{14}C, total C, and total N. Radiocarbon values were measured on the Van de Graaff FN accelerator mass spectrometer (AMS) at the Center for Accelerator Mass Spectrometry, Lawrence Livermore National Laboratory, Livermore California. In preparation for AMS analysis, samples were combusted in evacuated, sealed tubes in the presence of CuO and Ag, then reduced to graphite coating on iron powder in the presence of H2 (Vogel et al. 1984). Splits of combusted sample were taken for ^{13}C analysis from each organic and mineral horizon for correction of mass-dependent fractionation in the reported radiocarbon values. Whereas in other EBIS research reports radiocarbon values are presented as $\Delta^{14}C$ (‰), here we use % modern absolute, in keeping with previous DyDOC work (Michalzik et al. 2003; Tipping et al. 2005, Tipping et al. 2007); 100% modern absolute is equivalent to $\Delta^{14}C = 0‰$.

To date, the EBIS project has produced information on carbon balance and dynamics in the O-horizon (Hanson et al. 2005) and mineral soil (Swanston et al. 2005), CO_2 release by soil respiration (Cisneros-Dozal et al. 2006), DOM transport (Jardine et al. 2006; Fröberg et al. 2007a, 2009), root and bud C turnover (Joslin et al. 2006; Riley et al. 2009; Gaudinski et al. 2009), and fungal use of litter carbon (Treseder et al. 2006).

Model description

The model version used here, DyDOC-04, is a site-specific adaptation of earlier versions (Michalzik et al. 2003; Tipping et al. 2005, 2007). It differs in its hydrological sub-model and soil organic pools, the nomenclature for which has been modified. We previously postulated soil C fractions that were in part model constructs, i.e. not directly observable, but the large amount of data available from the EBIS project permitted the model C pools to be aligned more closely with measured values. In particular, we attempted to account explicitly for the low-density and dense fractions of the mineral soil. We changed the nomenclature with regard to DOM. Whereas in previous work, it had been assumed that there were two "humic" fractions HUM1 and HUM 2, we now prefer the nomenclature PDOM1 and PDOM2, by which is meant potential DOM in fractions 1 (more hydrophilic) and 2 (more hydrophobic). The point of the adjective "potential" is to take into account the fact that in some circumstances (notably the mineral soil) much of the hydrophobic fraction (and possibly some of the hydrophilic) will be sorbed to soil solids and therefore will not be dissolved, but it is considered able to participate in solid-solution partitioning and so has the potential to become DOM. Although more general versions of the model would use Hor-1, -2 and -3 for the soil horizons, we consider it clearer to use the terminology O, A and B for ORR since they are clearly defined within the experimental data. The currency of the model is carbon (DOC, particulate organic carbon—POC, etc.), but we use SOM, POM (particulate organic matter) etc. to refer to the actual entities that contain the carbon.

Water entering the soil is rainfall minus interception losses, which are estimated by assuming the fractional loss of water to decrease with rainfall

amount, and to be greater during the period of leaf cover. The soil pore space comprises macropores, within which water drains downwards, and micropores, within which it is stationary. Water enters the O-horizon macropores and then may be absorbed into the micropores if they are incompletely filled. Solute exchange between macropore and micropore takes place by pseudo-diffusion, governed by an exchange coefficient. Maximum evaporation loss is calculated from the product of the air temperature and a constant. The actual loss depends upon the available water in the horizon, and a minimum fractional micropore volume (10% of the total) is maintained. If there is space in the A-horizon macropore, some or all of the water in the O-horizon is transferred. Transfer to micropores, solute exchange and evaporation then take place as in the O-horizon. Drainage from the A-horizon depends upon the available macropore space in the B-horizon, and is also governed by a first-order drainage rate constant. The B-horizon operates in the same way as the A, except that drainage depends simply upon the macropore volume and the drainage rate constant, not on the available pore space at greater depth. Other versions of the model have allowed bypass flow from the O-horizon to streamwater, but for the present sites we assumed the water to drain only vertically. This assumption is supported by experimental observations on the ORR that suggest the lateral stormflow zone in these studies occurs at approximately 120 cm which is below the depth of observation in the present study (Wilson et al. 1993).

Figure 1 shows the soil organic matter pools assumed in DyDOC-04, and their inputs and outputs. Carbon enters the O-horizon as above- and below-ground litter, which decomposes to CO_2 or is transformed into SOM or PDOM, each process being characterised by a first-order rate constant. The SOM can either decompose to CO_2 or be converted to the two PDOM pools, again by first-order processes. The PDOM is lost from the O-horizon by mineralisation or by leaching. The A- and B-horizons have a common metabolic scheme. Carbon enters as root litter or DOM. The litter is transformed to either CO_2 or SOM1, equated to the observed low-density fraction. The DOM fractions may sorb to the soil solids (see below). The SOM2 pool is in close association with mineral matter, and may be formed from sorbed PDOM or SOM1, as indicated by the

dotted lines in Fig. 1. Together, sorbed PDOM and SOM2 constitute the observed high-density fraction. All the first-order metabolic transformations have a temperature dependence given by a Q_{10} relationship, i.e. the factor $Q_{10}^{(T/10)}$ is used to modify the first order rate constant, where T is the temperature in °C.

The PDOM fractions sorb to soil solids according to simple partitioning reactions, governed by K_D values. The sorption model does not include a capacity factor since the sorption process is assumed linear. Pool $PDOM_1$ is hydrophilic, $PDOM_2$ is hydrophobic, and this implies that K_{D1} is less than K_{D2} since it has been shown that hydrophobic PDOM fraction is preferentially sorbed by soil solid phase material relative to hydrophilic PDOM (e.g. Jardine et al. 1989, 2006).

Data sources for modelling

The EBIS study itself, together with much previous work at the site, has provided a wealth of data that we have used in the modelling effort. Much of this information has been reported elsewhere (see references given above), while the rest is available from long-term monitoring at the sites or unpublished information from the EBIS project (contact P. J. Hanson via http://ebis.ornl.gov for access).

DyDOC is driven by inputs of daily temperature and rainfall, litter, and the ^{14}C content of the litter. Daily meteorological data, including temperature data at several soil depths, were available for the years 1993–2005 inclusive. For earlier years we used the same data, repeated over time from the starting year of the model runs (usually 1000 AD). The model thus assumes a steady-state, but with a 13-year period inter-annual variation.

For steady-state conditions, we assumed a constant input of above-ground litter of 4.79 gC m^{-2} day^{-1} during the period 15 October to 1 December, and constant rates of input of root litter of 0.190, 0.193 and 0.086 gC m^{-2} day^{-1} for the O-, A- and B-horizons, respectively, during the period April to October inclusive. These correspond to the annual average values (Joslin and Wolfe 2003). The amounts entering were assumed to be the same in each year, except for the years of the study, for which the experimental above-ground litter inputs were used. Thus in 2000 no above-ground litter was applied, while

230 gC m^{-2} was applied on 15 May 2001, 15 January 2002, and 15 January 2003, after which natural inputs resumed.

Carbon contents were determined for the O-horizon as described by Hanson et al. (2005), and for the A- and B-horizons according to Swanston et al. (2005). Data for carbon contents of density-fractionated soil at TVA and WB were taken from Swanston et al. (2005) and at WB from Gaudinski and Trumbore (2003). Because these two sets of authors did not use the same fractionation procedure, we combined their findings. The adopted low-density fractions were taken to be the measured low-density fractions of Gaudinski and Trumbore, but the combined measured "free light" and "occluded light" fractions of Swanston et al., while the adopted high-density fractions were measured high-density fractions of Gaudinski and Trumbore, and the measured "dense" fraction of Swanston et al.

Soil water samples were collected with lysimeters, and analysed for DOC as described by Jardine et al. (2006). Note that the deepest field lysimeters were located at 70 cm depth, whereas the assumed B-horizon in the present study extends only to 60 cm. We assume the same DOC concentrations for both depths.

For the time period covered by the experiments, above-ground litter ^{14}C was well-known, but this did not apply to the immediately preceding period, nor were direct measurements of root litter ^{14}C available. In previous applications of DyDOC, it was assumed that all litter produced in a given year has the same ^{14}C signature, set at the atmospheric value for between zero (for moorland) and five (spruce forest) years earlier. However, the present study deals with shorter time scales, in particular the large atmospheric ^{14}C pulse during 1999, and so more precise estimation of litter ^{14}C was needed. Furthermore, Joslin et al. (2006) showed that root turnover at ORR is biphasic, occurring timescales of less than 1 year and of several years. Therefore, to take this into account, and also to estimate the ^{14}C input during the main pulse year of 1999, we constructed a simple steady-state model of carbon uptake by trees, and allocation of C within the plants and subsequent litter. The tree model was parameterised by fitting to available ORR data on root biomass and ^{14}C contents, and is fully described in the Electronic Supplementary Material. The parameterised tree model was used to estimate all annual litter ^{14}C contents for the period
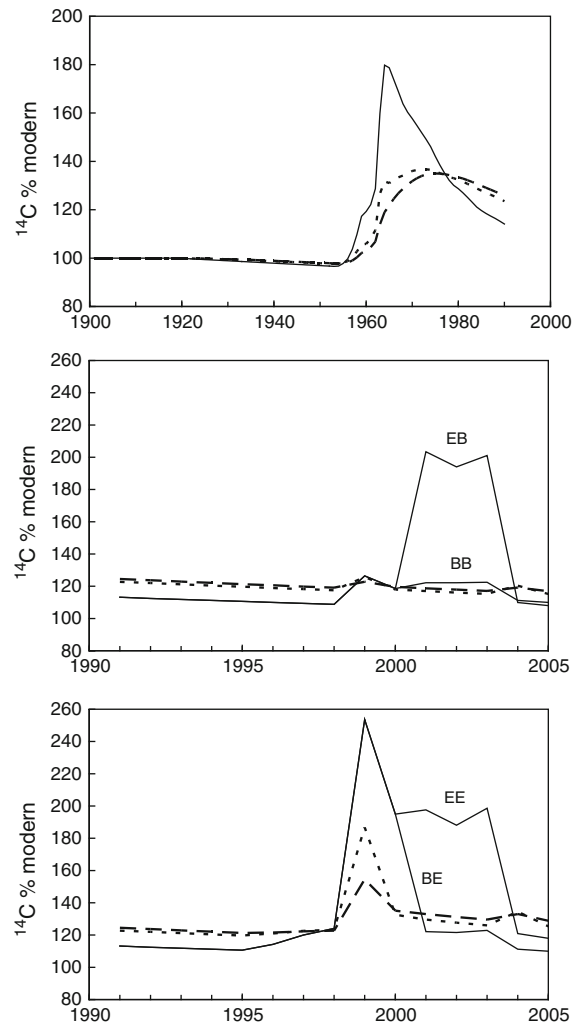

Fig. 2 Radiocarbon inputs to the ORR soil inferred from field observations and model fitting approximations. *Upper panel* 1900–1990, *lower panels* 1991–2005. *Solid lines* represent above-ground litter, *short dashes* O-horizon root litter, *long dashes* A-horizon root litter. The values for B-horizon roots, omitted for clarity, are similar to those for the A-horizon

1900–2006. The ^{14}C input data used for the different sites and treatments derived in this way are shown in Fig. 2.

Model calibration

The two soil types at ORR (Inceptisol and Utlisol) differ somewhat in their drainage and DOM sorption properties (Jardine et al. 2006). However, the sizes and vertical distributions of their carbon pools, and the

measured DOC fluxes, are sufficiently similar to justify the simplifying assumption that, at the resolution of DyDOC, all four sites operate identically with respect to soil carbon cycling. Moreover the sites are sufficiently close to one another to permit the assumption of identical climatic and weather conditions, and they have closely similar vegetation and litter fall. Thus, the four sites and paired experimental manipulations provided unprecedented replicated measurements of carbon pools, fluxes and isotope behaviour for model calibration. The representative soil profile used for modelling comprised an O-horizon of thickness 3 cm, bulk density 0.1 g cm^{-3} and 46% C by weight, an A-horizon (15 cm, 1.0 g cm^{-3}, 2.3% C) and a B-horizon (45 cm, 1.0 g cm^{-3}, 0.49% C).

The DyDOC hydrological sub-model used rainfall and temperature as driving variables to describe interception losses, evaporation and drainage. Its parameters were optimised by comparison with measured soil moisture data and with outputs from more sophisticated physical models. Data from the tracer experiments with bromide were used to optimise the sub-model further. These calibrations are described in the Electronic Supplementary Material.

With the hydrological and solute exchange processes parameterised, we fitted DyDOC to the available C data. Fitting was conducted first for the O-horizon and subsequently for the mineral soil. The target data for fitting consisted of measured soil C pools and their ^{14}C contents, as well as annual DOC fluxes and DO^{14}C data. For the A- and B-horizons the fractionation of soil organic C between the low-and high-density fractions was taken into account.

Optimisation was performed with combined objective functions, comprised of the sums of the squared deviations between observed and simulated values, normalised by division by the observed values. The O-horizon objective function was constructed from; litter C (2001–2003), OeOa C (2001–2003), DOC flux (2002), litter ^{14}C (1972, 1998, 2001–2003), OeOa ^{14}C (1972, 1998, 2001–2005), DO^{14}C (2005). The A- and B-horizon objective functions were each constructed from; litter C (2001–2003), total soil C (2001), fraction of low-density C (average), DOC flux (2002–2003), litter ^{14}C (2001–2003), soil ^{14}C (2001–2004), low-density fraction ^{14}C (1972, 1998, 2001), high-density fraction ^{14}C (1972, 1998, 2001), DO^{14}C (2002–2003).

The value of Q_{10} was set to 2.0 for all first-order transformations, and recent dynamic observations derived from soil respiration data provide general support for this assumption Gu et al. (2008).

Results

Carbon pools, fluxes and ^{14}C

We fitted the model for the O-horizon using the two measured carbon pools, litter (Oi) and the combined Oe and Oa material, which correspond to the L and SOM pools in the model (Fig. 1). Because the O-horizon at ORR is relatively thin, the Oe and Oa layers are not separated in sampling. Both the Oi and OeOa pools were considered to be potential sources of DOC in water draining from the O-horizon. The thinness of the O-horizon meant that adsorption of PDOM, for typical K_D values (Michalzik et al. 2003; Tipping et al. 2005), was minimal, and so both K_{D1} and K_{D2} were set to zero. Thus, although fractionation of the DOM due to adsorption was considered in the mineral soil (see below), it was not found necessary to do this for the O-horizon.

In preliminary fitting it was found that the parameter $k_{PDOM-CO_2}$ was poorly defined, i.e. it could take on a wide range of values because compensatory adjustments in the other metabolic parameters could be made. Therefore, the value was fixed at 0.15 a^{-1}, based on the fitting of A-horizon data (see below). Similar fits were obtained whether the PDOM was assumed to come from L or SOM so we forced the rate constant to be the same for each. Table 1 shows the optimised values of the metabolic rate constants.

Table 1 First order metabolic rate constants (a^{-1}) for the O-horizon

| Process	Constant	Value
Loss of CO_2 from L	k_{L-CO_2}	0.20
Transformation of L to SOM	k_{L-SOM}	0.054
Transformation of L to PDOM1 and PDOM2	k_{L-PDOM}	0.020[a]
Loss of CO_2 from SOM	$k_{SOM1-CO_2}$	0.016
Transformation of SOM to PDOM1 and PDOM2	$k_{SOM-PDOM}$	0.020[a]
Loss of CO_2 from PDOM	$k_{PDOM-CO_2}$	0.15[b]

[a] Constrained to be equal and [b] fixed

Table 2 Observed and simulated carbon pools (gC m^{-2}) and fluxes (gC m^{-2} a^{-1}) in the O-horizon

	Year	Observed	Simulated
Oi C pool	2001	202 (49)	230
	2002	245 (31)	264
	2003	366 (46)	244
OeOa C pool	2001	521 (105)	518
	2002	614 (122)	517
	2003	465 (112)	519
DOC flux	2002	46	46

The observed pools are means over all eight experimental plots with standard deviations in brackets, and refer to sampling performed in January for Oi and in October for OeOa. The DOC flux is the average of data from lysimeters at all four sites (HR, PR, TVA, WB)

Observed and simulated pools and DOC flux for the O-horizon are shown in Table 2, while Fig. 3 shows soil ^{14}C values over time. Four samples of O-horizon DOC were taken for the measurement of DO^{14}C during the study, all in 2005 at the BB and EB plots. The simulated value for BB in 2005 was 115.8% modern, in agreement with the observed values of 116.1 and 118.7% modern. For EB the simulated DO^{14}C of 135.3% modern agreed with one of the observations (140.0% modern), although less well with the other (166.3% modern), consistent with the rapid formation and leaching of DOM in the O-horizon.

The model fitting did not make use of short-term variability in DOC concentration or flux, only the

Fig. 3 Observed and simulated ^{14}C in the Oi (*upper graphs*) and OeOa horizon (*lower graphs*) for each of the four treatment manipulations
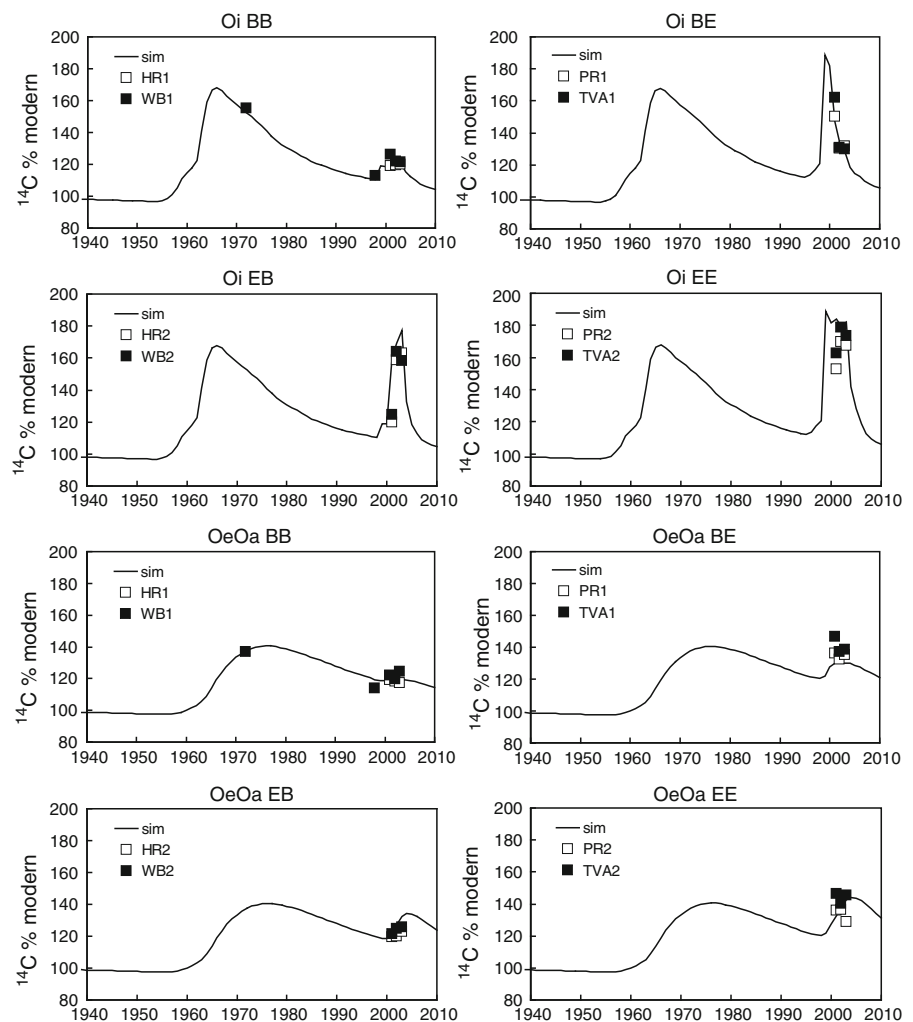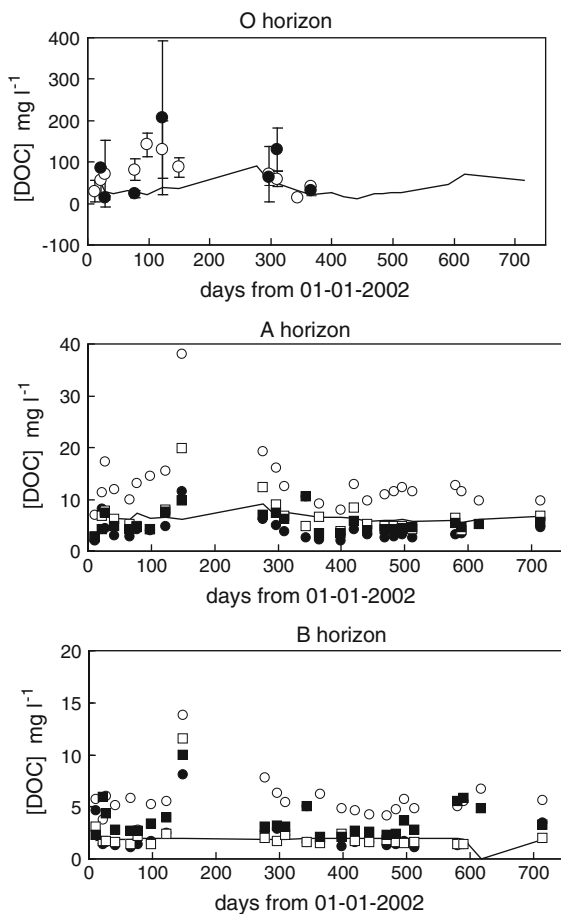
Fig. 4 Observed and simulated DOC concentrations in water draining from the O, A and B horizons. In the *top panel*, *standard errors* are shown, and the different *symbols* indicate different collectors depths within the O-horizon. The different *symbols* in the *lower two panels* refer to HR (*open circle*), PR (*filled circle*), TVA (*open square*), WB (*filled square*). *Standard errors* on these points were omitted for clarity, but ranged from 1 to 2 mg l^{-1}

annual flux. Although the annual flux was simulated well (Table 2), the model did not reproduce the high O-horizon DOC concentrations at the start of 2002, especially just before the dry period when samples were not retrieved (Fig. 4, top panel). The water flow events (Fig. S2) occurring between days 190 and 275 are important in the simulation, accounting for 47% of the total flux for 2002, whereas the corresponding measured flux occurs earlier, between days 70 and 140.

We parameterised horizons A and B simultaneously, optimising all 15 parameters shown in Table 3. Only at this point is it necessary to consider the fractions of PDOM separately, because they are assumed not to sorb to the O-horizon solids. Therefore f_{PDOM1} was optimised as part of the A–B parameterisation. We also optimised the sorption K_D values for PDOM1 and PDOM2, for simplicity assuming them to be the same for both the A- and B-horizons.

Alternative metabolic schemes in the mineral soil

The DOM entering the mineral soil from the O-horizon may adsorb to the soil solids, becoming part of the high-density fraction, or be lost by mineralisation to CO_2, or leached to lower depths. The only source of the low-density soil carbon fraction was assumed to be the root litter, but this fraction might also convert to the high-density fraction via microbial processing. We considered two metabolic schemes, I and II, as follows.

In Scheme I, the high-density fraction is derived only from DOM. For this to provide the correct high-density pool size and ^{14}C content, it has to be assumed that initially sorbed DOM is transformed to a different material, i.e. SOM2. Sorption alone cannot account for the accumulation of the high-density fraction, because the partition coefficients required to permit DOM to leach from the A- and B-horizons are too low to permit sufficient build-up of the sorbed pools. In Scheme II, SOM2 comes only from the SOM1 fraction. The two possibilities involve the same number of transformations, and therefore of parameters. In either case, the measured high-density fraction comprises sorbed PDOM1 and PDOM2, plus SOM2.

We excluded reactions that generate potential DOM in the mineral soil, because it is clearly a net sink for DOM (e.g. Jardine et al. 2006), which makes it impossible to quantify internal PDOC cycling. Similarly, it is not feasible to distinguish the mineralisation rates of sorbed and free DOM, although the sorbed fractions predominate, the main source of CO_2 being sorbed PDOM2.

The model was more successful when Scheme I assumptions were used. First, the sum of squared normalised deviations was smaller, by about a factor of two. Secondly the parameter values were more internally consistent. Table 3 shows that for Scheme I the values for the two horizons are fairly similar, in most cases the A-horizon value slightly exceeding

Table 3 Parameters for the A- and B-horizons

Process	Constant	Values for Scheme I		Values for Scheme II	
Fractionation of PDOM	f_{PDOM1}	0.064		0.095	
Sorption of PDOM	$K_{D,PDOM1}$	5.0×10^{-6}		5.8×10^{-6}	
	$K_{D,PDOM2}$	1.4×10^{-4}		1.6×10^{-4}	
		A-horizon	B-horizon	A-horizon	B-horizon
Loss of CO_2 from (root) litter	k_{L-CO_2}	0.016	0.0087	0.022	0.00062
Transformation of L to SOM1	k_{L-SOM1}	0.14	0.086	0.12	0.093
Loss of CO_2 from SOM1	$k_{SOM1-CO_2}$	0.013	0.013	0.010	0.030
Loss of CO_2 from PDOM	$k_{PDOM-CO_2}$	0.15	0.023	0.14	0.015
Transformation of PDOM to SOM2	$k_{PDOM-SOM2}$	0.034	0.057	n/a	n/a
Transformation of SOM1 to SOM2	$k_{SOM1-SOM2}$	n/a	n/a	0.0021	0.029
Loss of CO_2 from SOM2	$k_{SOM2-CO_2}$	0.0024	0.0013	0.0020	0.0027

The first order rate constants (k) have units of a^{-1}, the partition coefficients (K_D) are in $m^3 \, g^{-1}$. See the text for explanation of Schemes I and II

Table 4 Observed and simulated (Scheme I) carbon pools (gC m^{-2}) and fluxes (gC m^{-2} a^{-1}) in the A- and B-horizons

	A-horizon		B-horizon	
	Observed	Simulated	Observed	Simulated
Litter C				
2001	97 (2)	88	59 (5)	60
2002	76 (2)	89	55 (8)	60
2003	103 (9)	88	76 (4)	59
SOC				
2001	2,120 (230)	2,070	1,300 (130)	1,240
Low-density fraction	~ 0.5	0.47	0.36	0.33
DOC flux				
2002	7.6	7.1	1.9	1.4
2003	8.3	6.9	2.3	1.8

The observed values are means with standard deviation in brackets over all eight experimental plots (except for the low-density fraction). The DOC flux is an aggregation of data from lysimeters at all four sites (HR, PR, TVA, WB)

that for the B-horizon. However, for Scheme II k_{L-CO_2} and $k_{SOM1-SOM2}$ differ by more than a factor 10 between the two horizons, and the values of $k_{SOM1-CO_2}$ and $k_{PDOM-CO_2}$ also differ by more than their Scheme I versions.

The optimised values of $K_{D,PDOM1}$ and $K_{D,PDOM2}$ are similar for Schemes I and II, and are consistent with experimental values. Thus, if the sorption data of Jardine et al. (2006) at DOC concentrations similar to those in the field are fitted to simple partitioning reactions, the average K_D values for the different sites range between $1.6 \times 10^{-5} \, m^3 \, g^{-1}$ (Haw Ridge soil) and $8.1 \times 10^{-5} \, m^3 \, g^{-1}$ (Pine Ridge). The fitted values cover these ranges (Table 3), which is to be

expected given that DyDOC operates with two fractions that would be mixed in the experiments.

In view of the superiority of the Scheme I version of the model, i.e. in which SOM2 is derived entirely from PDOM, we show results only for this case. Table 4 compares observed and simulated C pools in A and B, and DOC fluxes. Figure 5 shows the variation of total soil ^{14}C over time, with clear bomb carbon incorporation but little evidence or simulation of enrichment by the recent atmospheric radiocarbon spike. The limited data available for the low- and high density ^{14}C contents (Fig. 6) are moderately well simulated, although differences between the sites mean that a faithful reproduction of the

Fig. 5 Observed and simulated total ^{14}C contents of the A and B horizons. Each *point* represents the mean of 2–4 replicates, with a typical standard deviation of 3%
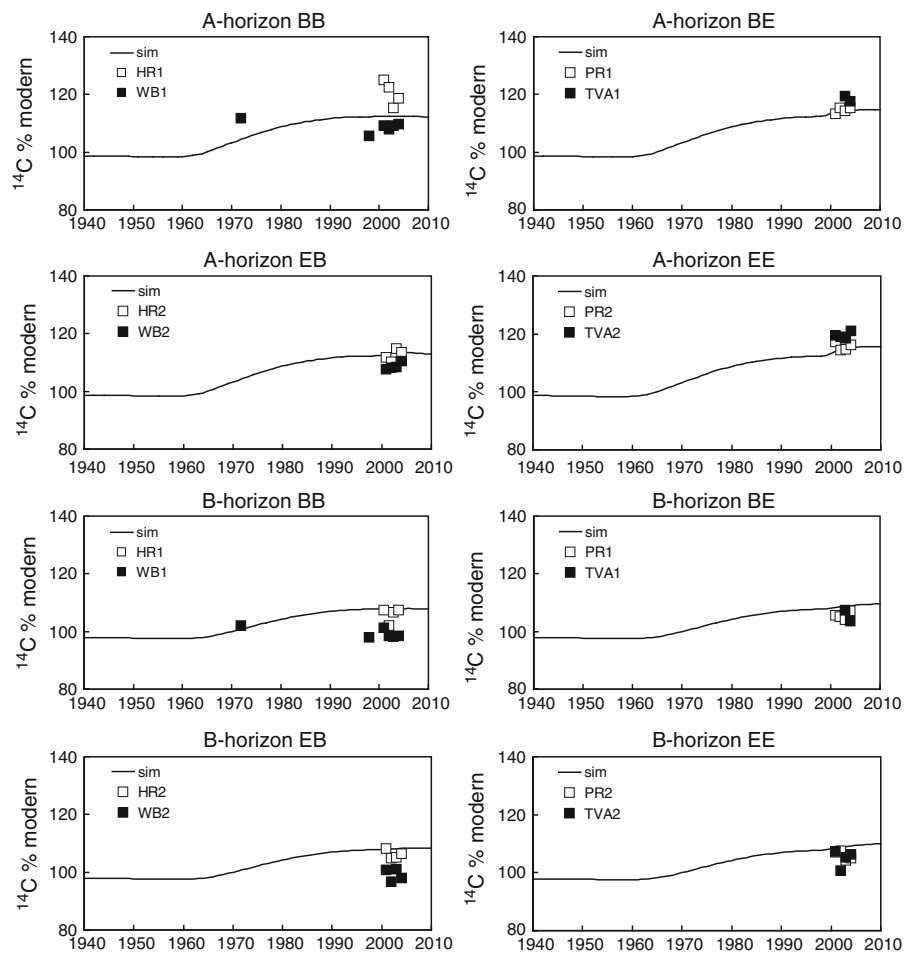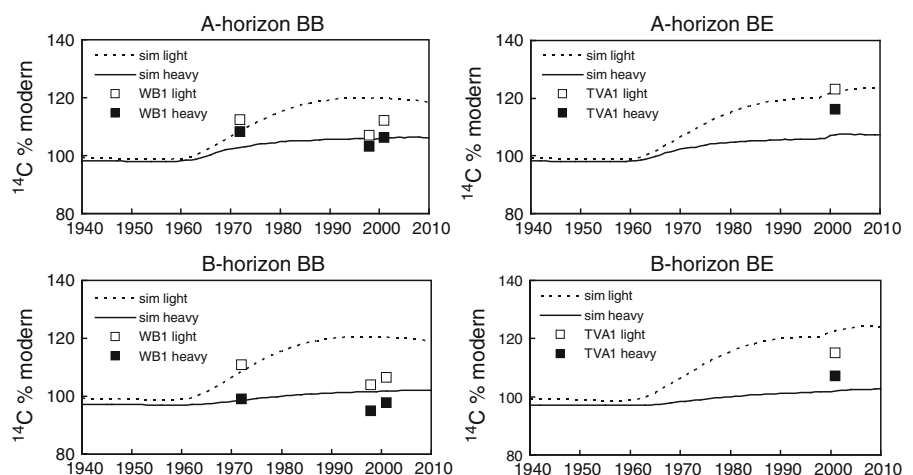

Fig. 6 Observed and simulated ^{14}C contents of the low- and high-density fractions of the A and B horizons. Each *point* represents the mean of 2–4 replicates, with a typical standard deviation of 3%


observations cannot be expected. Figure 7 shows that DO^{14}C in the mineral soil responded quite strongly to the input of enriched litter, and the model captures this behaviour.

Release of $^{14}CO_2$ from the soil

Cisneros-Dozal et al. (2006) measured the $^{14}CO_2$ release from soils at two of the four study sites

Fig. 7 Annual average observed and simulated DO^{14}C in drainage from the A and B horizons. Each *point* represents the mean of between 2 and 24 replicates, with an average standard deviation of 12%
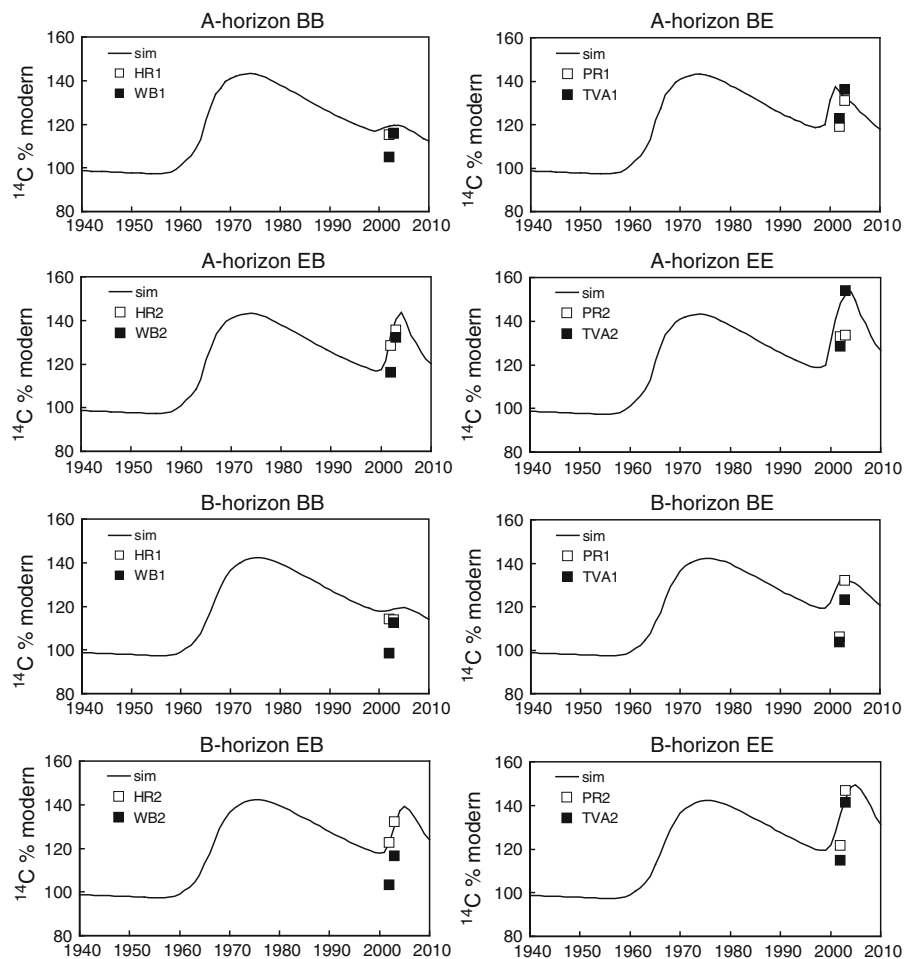
(Tennessee Valley Authority and Walker Branch) for both litter treatments, and apportioned the isotopic signal between plant and soil respiration. Thus, they derived values of $^{14}CO_2$ from the decomposition reactions that DyDOC seeks to simulate (although these data were not used in the model fitting). Figure 8 compares the observed and simulated $^{14}CO_2$ values, and shows good agreement between the different treatments, except that the model predicts a somewhat later decline in $^{14}CO_2$ from the O-horizon as decomposition of the enriched litter is completed. The simulated and observed values for $^{14}CO_2$ from the mineral soil both show a relatively small increase in the BE and EE cases, attributable to enriched root litter rather than to the above-ground litter additions.

Figure S4 shows the calculated daily contributions of the different soil horizons to the net heterotrophic

CO$_2$ release. The majority of soil respiration comes from the O-horizon above-ground litter.

Calculated pools and fluxes of C

The parameterised model was used to calculate the steady-state pools and annual fluxes of carbon in each of the three horizons, including the leaching transfers of DOC. This was done by averaging over the 13 years of available meteorological data. Mean residence times (MRT, year) were calculated by dividing the quantity of C in each pool (gC m^{-2}) by the steady-state flux (gC m^{-2} a^{-1}).

The modelled steady-state carbon balance (Fig. 9) shows that 83% of the carbon entering the O-horizon is lost as CO$_2$, while the remaining 17% leaves as DOM. Most of the CO$_2$ output is directly from the litter (L) pool (MRT 1.4 year), with a much smaller

Fig. 8 Observed (*points*) and simulated (*lines*) $^{14}CO_2$ released from the soil. *Open circles* and *thicker lines* represent the O-horizon, *closed circles* and *thinner lines* the mineral soil
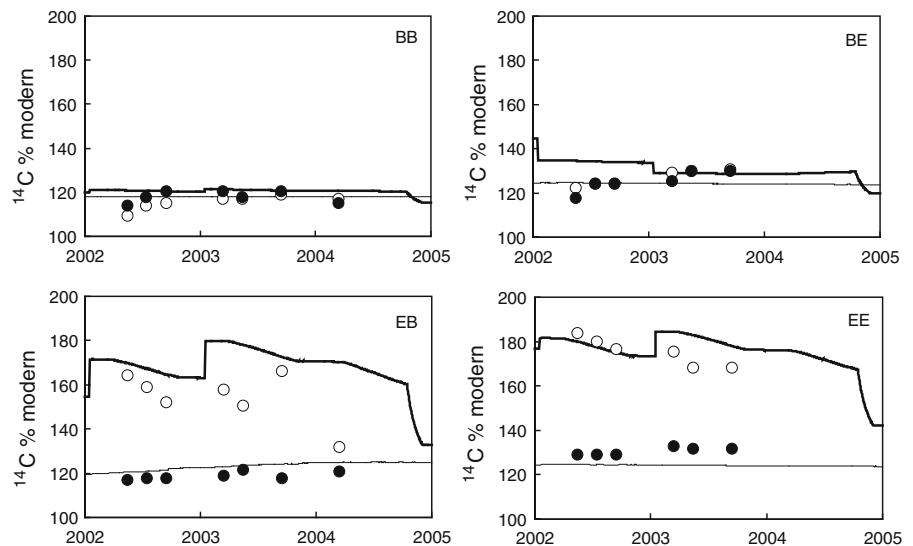
contribution from SOM (MRT 9.7 year), and minor mineralisation of PDOM. The overall MRT of C in the O-horizon is 3.3 year.

Approximately equal amounts of C enter the A horizon as root litter (40 gC m^{-2} a^{-1}) and DOM (46 gC m^{-2} a^{-1}), and in the preferred Scheme I they remain separate. Some root litter is mineralised directly to CO_2, but most is transformed to SOM1 (the low-density fraction), then returned as CO_2 with a MRT of 27 year. The DOM is retained first by adsorption then by transformation to SOM2$_A$ (MRT 140 year). The fate of root litter in the B-horizon is similar to that in the A. The B-horizon receives only 6 gC m^{-2} a^{-1}, but this feeds the stable SOM2$_B$ pool (MRT 200 year).

Considering the soil as a single carbon reservoir, the simplest measure of mean turnover time (total soil C/input) is only 13 years, but this conceals considerable heterogeneity, with modelled MRTs ranging from <1 to 200 year (see Fig. S5). The main source of CO_2 from the soil is the O-horizon litter pool, which contributes 61%, followed by the SOM1$_A$ (11%), the SOM$_O$ (7%) and SOM1$_B$ (5%). Only 0.3% of the total input C leaves as DOM from the B-horizon, representing about 3% of the DOC generated in the O-horizon. Therefore nearly all the DOM is ultimately lost by mineralisation, although some of its C persists in SOM2 for a century or more. This most stable form of soil C is due to the input of 11 gC m^{-2} a^{-1}, equivalent to only about 3% of total litter input, into SOM2$_A$ and SOM2$_B$.

According to the model DOM transported through the soil profile becomes more hydrophilic as downward movement occurs, which is consistent with field observations on the ORR (Jardine et al. 1990, 2006). The DOM leaving the O-horizon is 94% hydrophobic (Table 1), whereas that leaving the B-horizon is 83% hydrophilic. This reflects the weak sorption of PDOM1, which can therefore escape mineralisation, and explains the rapid appearance of the localised ^{14}C label in the A- and B-horizons at the EB and EE sites, i.e. those with enriched added litter (Fig. 7); see also Fröberg et al. (2007a, b).

Discussion

The DyDOC model is an assembly of plausible mechanisms of soil carbon dynamics, uniquely including DOM transport and retention in different horizons. Here, we modified previous versions of the model in order to utilise the greater amount and diversity of data available for ORR. In particular the EBIS study at ORR provided a wealth of ^{14}C values, and valuable data on the fractionation of mineral soil OM into low- and high-density fractions. Thus we have been able to address a key issue in soil carbon cycling, namely the heterogeneity of organic matter with respect to turnover rates.

The reasonable agreements between the DyDOC-04 simulations and the observations support the chosen mechanisms and their interactions. Furthermore, the
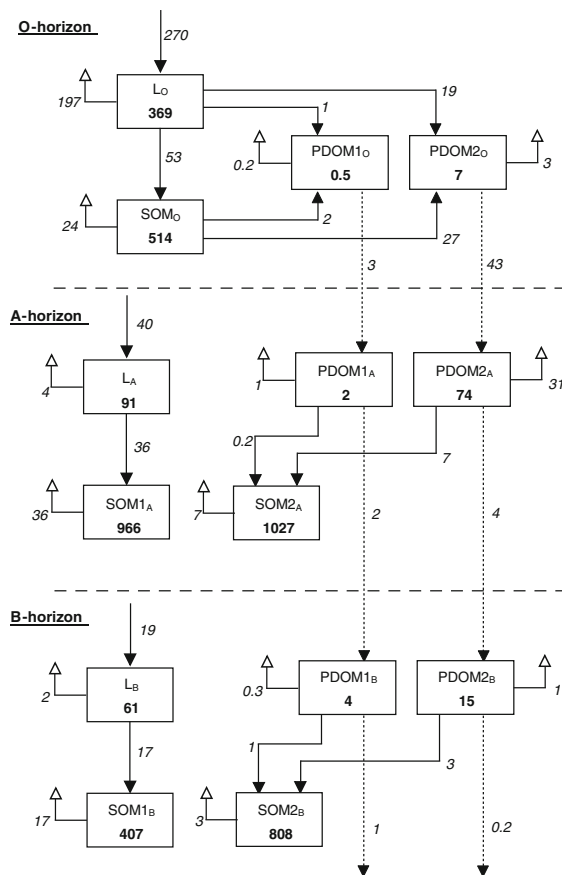
Fig. 9 Calculated steady state carbon pools (gC m^{-2}) and fluxes (gC m^{-2} a^{-1})

quantification of C turnover obtained with DyDOC did not use soil respiration $^{14}CO_2$ data, and so the fair agreement between predicted and observed values (Fig. 8) provides independent support for the model structure and parameterisation. With regard to model parameterisation, the availability of data arising from the short-term ^{14}C input spike proved especially valuable, providing information about short-term processes (O-horizon decomposition, DOM production and transport) while also demonstrating the relatively slow responses of mineral C pools.

O-horizon

Previous applications of DyDOC to coniferous forest and moorland soils (Michalzik et al. 2003; Tipping et al. 2005, 2007) showed that DOM leaching from O horizons comes from small fast-turnover pools. The

residence times of PDOM in the ORR O-horizon need to be particularly short (MRT $\sim$ 0.15 year) in order to explain the rapid labelling with ^{14}C in the EE case following the local atmospheric spike (see "Results" section). Thus, there can be little sorptive retention of either hydrophilic or hydrophobic PDOM, which is consistent with the finding of Fröberg et al. (2009) that there was no retention in the OeOa horizon of DOM produced in Oi horizon in experimental mesocosm studies with ORR soils. A predominance of hydrophobic DOM in the O-horizon leachate is deduced by considering the A-horizon (see below).

The modelling results suggest that litter and SOM provide PDOM, in similar amounts (40:60%). From mesocosm experiments on the ORR system, Fröberg et al. (2009) found a DOC output from the O-horizon equivalent to 43 g m^{-2} a^{-1}, very similar to the field value of 46 g m^{-2} a^{-1} (Fig. 9), with a ratio of 60:40% in favour of litter. The key finding here is that both litter and SOM are substantial sources of DOM leached from the O-horizon at ORR. This contrasts with results for the O-horizons of spruce forest soils in Sweden (Fröberg et al. 2003, 2007a, b; Tipping et al. 2005) and beech-oak forest soil in Germany (Kalbitz et al. 2007), for which litter is appreciably less important.

The model fitting procedure minimises the difference between observed and simulated annual DOC flux from the O-horizon (the annual predicted flux agrees well with the observed value) but does not take account of short-term variations in [DOC]. The results in the upper panel of Fig. 4 show that the combination of PDOM generation and water flow assumed for the O-horizon underpredicts [DOC] during the first 150 days, while the results for the period between 300 and 400 days are in better agreement. The discrepancy arises because the production rate of PDOM is too low, this being compensated for in the overall fitting by a higher rate of production during the warmer subsequent period (days 150–300). This might indicate moisture controls on PDOM formation, a temperature dependence that differs from the assumed Q$_{10}$ of 2.0, or the priming effect of fresh litter (Kalbitz et al. 2007).

Mineral soil

The fitted model reproduces the ^{14}C contents of the A-horizon quite well, but slightly overestimates those

of the B-horizon (Fig. 5). The increased ^{14}C levels seen for the past 40 years are due to bomb carbon. Minor incorporation of ^{14}C associated with the recent isotopic enrichment of the ORR forest is predicted for the BE and EE treatments, but this would be too small to be evident in the observations.

The DyDOC simulations are better with Scheme I (see "Results" section) in which all the stable OM in the mineral soil, represented by the high-density fraction, is derived from DOM, while the low-density fraction (also referred to as particulate organic matter, POM; Golchin et al. 1994) originates only from root litter. Because the low-density fraction has a faster turnover rate it is calculated to be more enriched in bomb carbon although there is little predicted enrichment with the recent localised ^{14}C pulse (Fig. 6). The simulations agree with the observations in that the model predicts the ^{14}C content of the low-density fraction to be greater than that of the high-density fraction (Fig. 6), but the absolute values are not precisely reproduced. This may reflect a more complex set of transformations than postulated in the model, i.e. a less strict division of low- and high-density sources, but it should also be borne in mind that the fractionation process may only provide a partial functional distinction of the soil carbon.

The nature of mineral soil organic matter postulated by the model agrees with evidence provided by Buurman and Jongmans (2005) that mineral soil SOM is either polymorphic (derived from root litter via mesofauna) or monomorphic (coatings on mineral matter, derived from DOM). These two types might correspond to the low- and high-density fractions, i.e. SOM1 and SOM2. Certainly adsorbed OM derived from DOM must be in the high-density fraction, and the low-density fraction can only have come from root litter, but it is less sure that root litter and its products should remain entirely in the low-density fraction, and not form any associations with mineral matter. Other recent papers promoting the idea of DOM as a source of stable mineral soil OM include those of Baisden and Parfitt (2007) and Sanderman and Amundson (2009). Rumpel et al. (2004) reported that the most stable (measured by ^{14}C) mineral soil C was in the smallest size fractions, which is also consistent with the stabilisation of dissolved organic matter. Mikutta et al. (2006) used chemical extractions to distinguish stable and not/unstable SOM from mineral soils. The readily oxidised fraction in most of

the soils was young according to ^{14}C (9 of the 13 examples contained bomb carbon). The stable fraction had a ^{14}C age ranging from 75 to 6,350 years (average 2,095 years) and was mainly (73% on average) associated with minerals. The minor part of the stable fraction was molecularly recalcitrant. Our model pools correspond to the first two of these three classes, the turnover time of stabilised SOM at ORR being at the lower end of the Mikutta et al. values.

A second assumption about PDOM in the mineral soil is that the adsorbed material somehow "matures" over time, rendering it permanently immobilised, but able to undergo mineralisation to CO_2. This process, which might be considered humification, is necessary because if only simple adsorption is permitted, coupled with mineralisation of the adsorbed PDOM, the model cannot build up much stabilised carbon in the mineral soil. With no mineralisation, an adsorption steady-state is reached with equal input and output [DOC], and the mineral horizon is not a sink for incoming DOM. But if the mineralisation rate is increased to make the horizon a sink, then only a small adsorbed pool can exist at steady-state, corresponding to the prevailing soil solution [DOC]. The putative maturing reaction, characterised by $k_{PDOM\text{-}SOM2}$, permits build up of stabilised OM to occur, while allowing a relatively small sorbed pool and maintaining the mineralisation rate, hence making the A-horizon both a net sink and a repository for stabilised C. As noted in "Results" section, transformation to SOM2 is a small flux that maintains a relatively large, pool, turning over slowly. Direct evidence for the formation of SOM2 in field soil is lacking in the literature, although in experimental studies (abiotic) polymerisation reactions have been shown to occur at mineral surfaces (Shindo and Huang 1982). Other maturing processes could include dehydration, and the slow transfer of sorbed molecules to rare high-energy sites on the mineral sorbents.

Summary and conclusions

The derived steady-state C pools and fluxes summarised in Fig. 9 provide a detailed quantitative description of soil C cycling in the ORR deciduous forest soil profile. They demonstrate the role of DOM in the turnover of carbon in the O-horizon, and the

formation and turnover of SOM in the mineral soil. We find that the pool of potential DOM in the O-horizon turns over rapidly, so that leached DOM is fresher than that leaving the O-horizons of coniferous forests. Of the mainly hydrophobic DOC entering the mineral soil each year, a small amount of predominantly hydrophilic material escapes in solution from the B-horizon. The bulk of the percolating DOM is initially removed by adsorption, then most is removed by conversion to CO_2, but a small amount is transformed into a more stable form of SOM, thereby feeding the most stable SOM pools. These conclusions represent the most internally consistent interpretation of the data provided by the model. The parameterised model can be regarded as a formal hypothesis about soil carbon dynamics in ecosystems like that at ORR, and is open to testing by further experiments and field monitoring. In particular there is a need to investigate the maturing reaction postulated to occur following DOM sorption.

References

Amundson R (2001) The carbon budget in soils. Annu Rev Earth Planet Sci 29:535–562

Baisden WT, Parfitt RL (2007) Bomb ^{14}C enrichment indicates decadal C pool in deep soil? Biogeochemistry 85:59–68

Buurman P, Jongmans AG (2005) Podzolisation and soil organic matter dynamics. Geoderma 125:71–83

Cisneros-Dozal LM, Trumbore S, Hanson PJ (2006) Partitioning sources of soil-respired CO_2 and their seasonal variation using a unique radiocarbon tracer. Glob Change Biol 12:194–204

Fröberg M, Berggren D, Bergkvist B, Bryant C, Knicker H (2003) Contributions of Oi, Oe and Oa horizons to dissolved organic matter in forest floor leachates. Geoderma 113:311–322

Fröberg M, Jardine PM, Hanson PJ, Swanston CW, Todd DE, Tarver JR, Garten CT (2007a) Low dissolved organic carbon input from fresh litter to deep mineral soils. Soil Sci Soc Am J 71:347–354

Fröberg M, Berggren Kleja D, Hagedorn F (2007b) The contribution of fresh litter to dissolved organic carbon leached from a coniferous forest floor. Eur J Soil Sci 58:108–114

Fröberg M, Hanson PJ, Trumbore SE, Swanston CW, Todd DE (2009) Flux of carbon from ^{14}C-enriched leaf litter throughout a forest soil mesocosm. Geoderma 149: 181–188

Gaudinski JB, Trumbore SE (2003) Soil carbon turnover. In: Hanson PJ, Wullschleger SD (eds) North American temperate deciduous forest responses to changing precipitation regimes. Springer, New York

Gaudinski JB, Torn MS, Riley WJ, Swanston C, Trumbore SE, Joslin JD, Majdi H, Dawson TE, Hanson PJ (2009) Use of stored carbon reserves in growth of temperate tree roots and leaf buds: analyses using radiocarbon measurements and modelling. Global Change Biol 15:992–1014

Golchin A, Oades JM, Skjemstad J, Clarke P (1994) Soil structure and carbon cycling. Aust J Soil Res 32: 1043–1068

Gu L, Hanson PJ, Post WM, Liu Q (2008) A novel approach for identifying the true temperature sensitivity from soil respiration measurements. Glob Biogeochem Cycles 22:GB4009. doi:10.1029/2007GB003164

Guggenberger G, Zech W (1992) Retention of dissolved organic carbon and sulfate in aggregated forest soils. J Environ Qual 21:643–653

Hagedorn F, Saurer M, Blaser P (2004) A C-13 tracer study to identify the origin of dissolved organic carbon in forested mineral soils. Eur J Soil Sci 55:91–100

Hanson PJ, Wullschleger SD (eds) (2003) North American temperate deciduous forest responses to changing precipitation regimes. Ecological studies, vol 166. Springer, New York, 472 pp

Hanson PJ, Swanston CW, Garten CT, Todd DE, Trumbore SE (2005) Reconciling change in Oi-horizon carbon-14 with mass loss for an oak forest. Soil Sci Soc Am J 69: 1492–1502

Jardine PM, Wilson GV, Luxmoore RJ (1988) Modeling the transport of inorganic ions through undisturbed soil columns from two contrasting watersheds. Soil Sci Soc Am J 52:1252–1259

Jardine PM, Weber NL, McCarthy. JF (1989) Mechanisms of dissolved organic carbon adsorption by soil. Soil Sci Soc Am J 53:1378–1385

Jardine PM, Wilson GV, McCarthy JF, Luxmoore RJ, Taylor DL (1990) Hydrogeochemical processes controlling the transport of dissolved organic carbon through a forested hillslope. J. Contam Hydrol 6:3–19

Jardine PM, Mayes MA, Mulholland PJ, Hanson PJ, Tarver JR, Luxmoore RJ, McCarthy JF, Wilson GV (2006) Vadose zone flow and transport of dissolved organic carbon at multiple scales in humid regimes. Vadose Zone J 5:140–152

Jenkinson DS (1990) The turnover of organic carbon and nitrogen in soil. Philos Trans R Soc B 329:361–368

Jenkinson DS, Coleman K (2008) The turnover of organic carbon in subsoils. Part 2. Modelling carbon turnover. Eur J Soil Sci 59:400–413

Johnson DW, Van Hook RI (eds) (1989) Analysis of biogeochemical cycling processes in Walker Branch Watershed. Springer, New York

Joslin JD, Wolfe MH (2003) Fine root growth response. In: Hanson PJ, Wullschleger SD (eds) North American temperate deciduous forest responses to changing precipitation regimes. Ecological studies, vol 166. Springer, New York, pp 274–302

Joslin JD, Gaudinski JB, Torn MS, Riley WJ, Hanson PJ (2006) Fine-root turnover patterns and their relationship to root diameter and soil depth in a C-14-labelled hardwood forest. New Phytol 172:523–535

Kaiser K, Zech W (1997) Competitive sorption of dissolved organic matter fractions to soils and related mineral phases. Soil Sci Soc Am J 61:64–69

Kalbitz K, Kaiser K (2008) Contribution of dissolved organic matter to carbon storage in forest mineral soils. J Plant Nutr Soil Sci 171:52–60

Kalbitz K, Schwesig D, Rethemeyer J, Matzner E (2005) Stabilization of dissolved organic matter by sorption to the mineral soil. Soil Biol Biochem 37:1319–1331

Kalbitz K, Meyer A, Yang R, Gestberger P (2007) Response of dissolved organic matter in the forest floor to long-term manipulation of litter and throughfall inputs. Biogeochemistry 86:301–318

Luxmoore RJ, Huff DD (1989) Water. In: Johnson DW, Van Hook RI (eds) Analysis of biogeochemical cycling processes in walker branch watershed. Springer, New York

Michalzik B, Tipping E, Mulder J, Gallardo Lancho JF, Matzner E, Bryant CL, Clarke N, Lofts S, Vicente Esteban MA (2003) Modelling the production and transport of dissolved organic carbon in forest soils. Biogeochemistry 66:241–264

Mikutta R, Kleber M, Torn MS, Jahn R (2006) Stabilization of soil organic matter: association with minerals or chemical recalcitrance? Biogeochemistry 77:25–56

Neff JC, Asner GP (2001) Dissolved organic carbon in terrestrial ecosystems: synthesis and a model. Ecosystems 4:29–48

Parton WJ, Schimel DS, Cole CV, Ojima DS (1987) Analysis of factors controlling soil organic levels of grasslands in the Great Plains. Soil Sci Soc Am J 51:1173–1179

Parton WJ, Hartman M, Ojima D, Schimel D (1998) DAYCENT and its land surface submodel: description and testing. Glob Planet Change 19:35–48

Qualls RG, Haines BL (1991) Geochemistry of dissolved organic nutrients in water percolating through a forest ecosystem. Soil Sci Soc Am J 55:1112–1123

Qualls RG, Haines BL (1992) Biodegradability of dissolved organic nutrients in forest throughfall, soil solution, and stream water. Soil Sci Soc Am J 56:578–586

Riley WJ, Gaudinski JB, Torn MS, Joslin JD, Hanson PJ (2009) Fine-root mortality rates in a temperate forest: estimates using radiocarbon data and numerical modelling. New Phytol 184:387–398

Rumpel C, Eusterhues K, Kögel-Knabner I (2004) Location and chemical composition of stabilized organic carbon in topsoil and subsoil horizons of two acid forest soils. Soil Biol Biochem 36:177–190

Sanderman J, Amundson R (2009) A comparative study of dissolved organic carbon transport and stabilization in California forest and grassland soils. Biogeochemistry 92:41–59

Shindo H, Huang PM (1982) Role of Mn(IV) oxide in abiotic formation of humic substances in the environment. Nature 298:363–365

Swanston CW, Torn MS, Hanson PJ, Southon JR, Garten CT, Hanlon EM, Ganio L (2005) Initial characterization of processes of soil carbon stabilization using forest stand-level radiocarbon enrichment. Geoderma 128:52–62

Tipping E, Fröberg M, Berggren D, Mulder J, Bergqvist B (2005) DOC leaching from a coniferous forest floor: modelling a manipulation experiment. J Plant Nutr Soil Sci 168:316–324

Tipping E, Smith EJ, Bryant CL, Adamson JK (2007) The organic carbon dynamics of a moorland catchment in N.W. England. Biogeochemistry 84:171–189

Treseder KK, Torn MS, Masiello CA (2006) An ecosystem-scale radiocarbon tracer to test use of litter carbon by ectomycorrhizal fungi. Soil Biol Biochem 38:1077–1082

Trumbore SE (2000) Age of soil organic matter and soil respiration: radiocarbon constraints on belowground C dynamics. Ecol Appl 10:399–411

Trumbore SE (2009) Radiocarbon and soil dynamics. Annu Rev Earth Planet Sci 37:47–66

Trumbore SE, Gaudinski JB, Hanson PJ, Southon JR (2002) Quantifying ecosystem-atmosphere carbon exchange with a ^{14}C label. EOS 83(265):267–268

Vogel JS, Southon JR, Nelson DE, Brown TA (1984) Performance of catalytically condensed carbon for use in accelerator mass-spectrometry. Nucl Instrum Methods Phys Res B 5:289–293

Wilson GV, Luxmoore RJ (1988) Infiltration, macroporosity, and mesoporosity distributions in two forested watersheds. Soil Sci Soc J Am 52:329–335

Wilson GV, Jardine PM, O'Dell JD, Collineau M (1993) Field-scale transport from a buried line source in unsaturated soil. J Hydrol 145:83–109